Journal of Magnetism and Magnetic Materials 463 (2018) 7–12

Contents lists available at ScienceDirect

Journal of Magnetism and Magnetic Materials

journal homepage: www.elsevier.com/locate/jmmm

Research articles

Nitrogen concentration induced spin disorder in ε-iron nitrides

Liyong Yuan [a,b], Hao Pan [b], Qisong Sun [b], Wenkun Tuo [a], Guoke Li [a,*], Liyun Jia [b], Ruibin Zhao [b], Junjie Shen [a], Li Ma [b], Congmian Zhen [b], Denglu Hou [b]

[a] Department of Mathematics and Physics, Institute of Applied Physics, Shijiazhuang Tiedao University, Shijiazhuang 050043, People's Republic of China
[b] Department of Physics, Hebei Advanced Thin Films Laboratory, Hebei Normal University, Shijiazhuang 050024, People's Republic of China

ARTICLE INFO

Article history:
Received 11 October 2017
Received in revised form 16 April 2018
Accepted 5 May 2018
Available online 7 May 2018

Keywords:
ε-Iron nitride
Bloch-Grüneisen formula
Electron-magnon scattering
Magnetoresistance

ABSTRACT

The magnetic and transport properties of ε-$Fe_{3-x}N$ ($0 \le x \le 1$) films were systematically characterized to identify the correlation among the nitrogen concentration x, magnetic structure, and electrical transport properties. It was found that increasing the nitrogen concentration x of ε-$Fe_{3-x}N$ not only resulted in a successive decrease in magnetization and Curie temperature, but also led to the contribution of magnetic scattering to the resistivity and magnetoresistance. All these experimental phenomena can be attributed to the distinctive exchange interaction in ε-$Fe_{3-x}N$, which depends on the concentration and distribution of nitrogen atoms and causes the emergence of localized spin disorder. We believe this work would provide a new insight into the relationship between the magnetic and transport properties of iron nitrides.

1. Introduction

Iron nitrides have received considerable scientific and technological attention because of their extreme hardness, chemical inertness, good electrical conductivity and excellent magnetic properties [1–4]. Among the various crystalline phases in the Fe-N phase diagram, ε-iron nitride, with general formula ε-$Fe_{3-x}N$ ($0 \le x \le 1$), is notable for occurring over a broad non-stoichiometric composition regime [5]. Throughout the entire compositional range of ε-$Fe_{3-x}N$, the Fe atoms maintain a slightly distorted *hcp* sublattice, and the N atoms tend to form ordered arrays in the interstitial sites with maximum separation [6]. Nevertheless, except for stoichiometric ε-Fe_3N and ε-Fe_2N, i.e. the two opposite limiting compositions of ε-$Fe_{3-x}N$, it is impossible for all the Fe atoms having an identical N atomic coordination number [7]. Magnetic measurements on powder samples revealed that both the Curie temperature and saturation magnetization of ε-$Fe_{3-x}N$ decreased drastically with increasing nitrogen concentration x [8–11]. The Mössbauer spectrums further indicated that the magnetic moments of Fe atoms were sensitive to the concentration and distribution of the N atoms in the lattice [12]. These results demonstrated the significant influence of nitrogen concentration on the magnetic properties of ε-$Fe_{3-x}N$, but there was a lack of reasonable explanation for these experimental phenomena.

To address this issue, extensive theoretical efforts have been devoted to investigate the influence of nitrogen concentration on the magnetic properties of ε-$Fe_{3-x}N$. The nearest-neighbor N donor model was insufficient to explain the rapid decrease of magnetization and Curie temperature in the composition range of ε-$Fe_{3-x}N$ [13–15]. The reduction of the magnetic moments of Fe with nitrogen concentrations in ε-$Fe_{3-x}N$ were highly underestimated by first principle calculation [16,17]. The widely used cell volume effect in interstitial compounds can also hardly explain the magnetic properties of ε-$Fe_{3-x}N$ [18,19]. So far, the correlation between the magnetic moments of Fe atoms and its N atomic coordination is still poorly understood, and no consensus has been reached on the exchange interaction in ε-$Fe_{3-x}N$. Moreover, most work on ε-$Fe_{3-x}N$ concentrated on the structure and magnetic properties [1,20–22], and there were only a limited number of reports on the transport properties of ε-$Fe_{3-x}N$ [23,24]. The correlation among nitrogen concentration x, magnetic properties, and electrical transport properties in ε-$Fe_{3-x}N$ has not been the object of systematic study. This is a serious deficiency since a deep understanding on the transport properties of ε-$Fe_{3-x}N$ is crucial for their applications in spintronics. Furthermore, the electronic transport properties, such as magnetoresistance (MR) and the Hall effect, may be taken as powerful tools to diagnose the magnetic structure [25,26]. If the magnetic and transport properties of ε-$Fe_{3-x}N$ are investigated together, the influence of nitrogen concentration on the magnetic structure and the transport properties might be clarified.

We have prepared ε-$Fe_{3-x}N$ over a wide range of compositions [18]. In this study, the magnetic and transport properties of this

* Corresponding author.
E-mail address: liguoke@126.com (G. Li).

https://doi.org/10.1016/j.jmmm.2018.05.017
0304-8853/

series of films were systematically analyzed, with the objective to establish the correlations among nitrogen concentration x, localized magnetic structures, and the electrical transport properties. A phenomenon mechanism of exchange interaction in ε-$Fe_{3-x}N$ is proposed according to the experimental results. The variations of saturation magnetization, Curie temperature, resistivity and MR with nitrogen concentration x can be simulated and interpreted simultaneously based on this mechanism. All these results reveal the fact that both the magnetic and transport properties are closely related to the concentration and microscopic distribution of N atoms in ε-$Fe_{3-x}N$.

2. Experimental

ε-$Fe_{3-x}N$ films were sputtered on AlN buffered glass substrates from a high purity Fe target [7,18]. The substrate temperature was kept at 350 °C and the base pressure of the chamber was better than 2.0×10^{-4} Pa. The total flow rate of Ar and N_2 gas mixtures was maintained at 50.0 sccm with sputtering pressure 1.0 Pa. The nitrogen content of the films was controlled by changing the nitrogen partial pressure which increased monotonically from 0.18 to 0.38 Pa in steps of 0.04 Pa. The film thickness, determined by X-ray Reflectivity, was 120 ± 5 nm for all the films [7]. The crystallinity of the films was characterized by X-ray diffraction (XRD). A physical property measurement system (PPMS-9, Quantum Design, Inc) was used to measure the magnetic and transport properties. For transport measurements, Hall bars were fabricated by using shadow masks of five terminals and the magnetoresistance (MR) was measured with the magnetic field applied perpendicular to the film.

3. Results

The XRD patterns of the films prepared under different nitrogen partial pressures are shown in Fig. 1(a). Comparing with standard powder XRD pattern on the bottom, it can be inferred that all the diffraction peaks belong to ε-$Fe_{3-x}N$ and the films have a polycrystalline structure. Moreover, the diffraction peaks move towards low angles with increasing nitrogen partial pressure, which means that the incorporation of N atoms into ε-$Fe_{3-x}N$ results in the expansion of the unit cell. As shown in Fig. 1(b), the derived lattice parameters increase monotonically with increasing nitrogen partial pressure. Comparing the lattice parameters with the results of Liapina et al. [27], who list the lattice parameter over the whole composition range of ε-$Fe_{3-x}N$, the derived nitrogen concentration

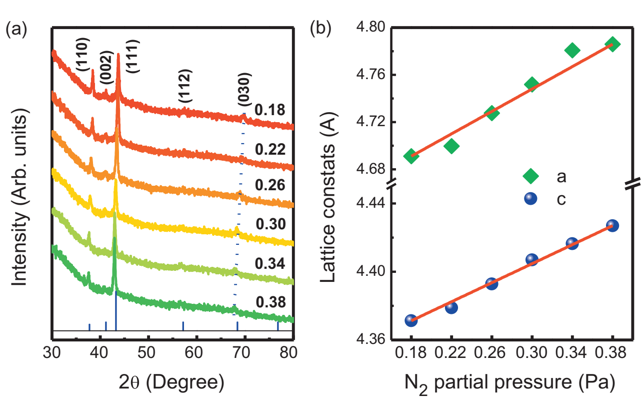

Fig. 1. (a) XRD patterns of the films prepared under different nitrogen partial pressures, and the blue lines on the bottom are the standard powder XRD pattern of ε-Fe_3N; (b) lattice parameters as a functions of nitrogen partial pressure determined from the diffraction peaks. The red solid lines are guide to eyes.

x in ε-$Fe_{3-x}N$ nearly increases linearly from 0.00 to 0.90 with increasing nitrogen partial pressure from 0.18 to 0.38 Pa. For convenience, the values of the nitrogen concentration x are also used to denote the films hereafter.

The temperature dependence of the magnetization with 1.0 kOe magnetic field in plane of the films is shown in Fig. 2(a). It can be inferred that both Curie temperature and magnetization decrease drastically with increasing nitrogen concentration. The Curie temperature for $x = 0.0$, 0.18, and 0.36 is well above 400 K, and the Curie temperatures for $x = 0.54$, 0.72, and 0.90 are about 320 K, 170 K and 90 K, respectively. The Curie temperature are shown as a function of nitrogen concentration x in Fig. 2(c). In addition, data points of ε-$Fe_{3-x}N$ powder samples cited from the literature are also provided to get the variation of the Curie temperature over whole composition range [8–11]. It can be seen that T_C decreases rapidly with increasing x, and drop to zero near the upper limit of ε-$Fe_{3-x}N$. The in plane hysteresis loops of the films measured at 10 K are displayed in Fig. 2(b). All of the films exhibit soft magnetic properties with coactivity less than 500 Oe. The saturation magnetizations decrease drastically from 1146 emu/cc to 96 emu/cc as x increased from 0.18 to 0.38, which is in excellent agree with the results of bulk samples. Considering that the main changes in ε-$Fe_{3-x}N$ are the number of N atomic coordinations for Fe atoms, the drastic reduction of magnetic properties highlights the significant influence of the nearest N neighbors on the exchange interaction between Fe atoms. Perhaps the nitrogen concentration also has a significant impact on the transport properties of ε-$Fe_{3-x}N$. Therefore, the transport properties, including the resistivity and MR, are systematically characterized.

The temperature dependence of the electrical resistivity ρ_{tot} for ε-$Fe_{3-x}N$ films is shown in Fig. 3. It is evident that all the films manifest characteristic metallic conductance irrespective of their nitrogen concentration. With increasing x, the resistivity increases gradually, whereas the profile of the curves has a marked change around 0.54. For the films with $x \leq 0.36$ (open black symbols), the resistivity approximately linearly decreases with decreasing temperature and reaches a constant value at low temperature. These films exhibit the characteristic of normal metal and thus the curves can be described by Bloch-Grüneisen formula [28]

$$\rho(T) = \rho_0 + \beta T\left(\frac{T}{\Theta_D}\right)^4 \int_0^{\Theta_D/T} \frac{x^5 dx}{(e^x - 1)(1 - e^{-x})}, \quad (1)$$

where ρ_0 is the residual resistivity, β is a constant, and Θ_D is the Debye temperature. The second term represents the electron-phonon scattering. The least-squares fitting results are shown by the blue solid lines in Fig. 3.

The curves with $x \geq 0.54$ (open pink symbols) are well different from those with $x \leq 0.36$. It can be seen from Fig. 3 the resistivity approximately follows the Bloch-Grüneisen formula at high temperature, while decays exponentially at low temperature. Based on this variation trend, an empirical term, $\rho_m = a\exp(-E_m/k_BT)$, which approaches a constant value at sufficiently high temperature and decreases exponentially at low temperature [29], is added to Bloch–Grüneisen formula. Then, the modified formula

$$\rho(T) = \rho_0 + \beta T\left(\frac{T}{\Theta_D}\right)^4 \int_0^{\Theta_D/T} \frac{x^5 dx}{(e^x - 1)(1 - e^{-x})} + a\exp(-E_m/k_BT), \quad (2)$$

reproduces the experimental results nicely, as shown by red solid lines in Fig. 3. It is clear that ρ_m increases sharply with both increasing of temperature and x. Considering the rapid decrease of T_C and m with increasing x, the emergence of ρ_m should be associated with the magnetic scattering.

The fitting parameters of both formula (1) for $x \leq 0.36$ and formula (2) for $x \geq 0.54$ are listed in Table 1. The notable features of